NMR Assignment and Secondary Structure Determination of an Octameric 110 kDa Protein Using TROSY in Triple Resonance Experiments

Michael Salzmann,[†,‡,§] **Konstantin Pervushin,**[†] **Gerhard Wider,**[†] **Hans Senn,**[‡] **and Kurt Wüthrich*,**[†]

Contribution from the Institut für Molekularbiologie und Biophysik, Eidgenössische Technische Hochschule Hönggerberg, CH-8093 Zürich, Switzerland, and F. Hoffmann-La Roche Ltd., Pharma Research, CH-4070 Basel, Switzerland

Received January 31, 2000. Revised Manuscript Received April 24, 2000

Abstract: TROSY-type triple resonance experiments with the uniformly ^{2}H,^{13}C,^{15}N-labeled 7,8-dihydroneopterin aldolase (DHNA) from *Staphylococcus aureus*, which is a symmetric homooctamer protein of molecular mass 110 kDa, showed 20-fold to 50-fold sensitivity gains when compared to the corresponding conventional triple resonance NMR experiments. On this basis, sequential connectivities could be established for nearly all pairs of neighboring residues in DHNA. TROSY-type nuclear Overhauser enhancement spectroscopy yielded additional data to close the remaining gaps in the sequential assignment, and provided supplementary information on the secondary structure. Complete sequence-specific assignments of the 121-residue polypeptide chain in this 110 kDa octamer could thus be obtained in aqueous solution at 20 °C, and the regular secondary structures in the solution conformation were found to coincide nearly identically with those in the crystal structure of the DHNA octamer.

Introduction

In nuclear magnetic resonance (NMR)[1] spectroscopy of biological macromolecules the assignment of chemical shifts to individual atoms provides the foundation for three-dimensional structure determination,[2] as well as, possibly in combination with structure determination by X-ray crystallography, for detailed studies of dynamic processes, interactions with other macromolecules in supramolecular structures, or studies of small-ligand binding.[3,4] To cite just a few types of studies that can be based on sequence-specific backbone assignments in proteins, the secondary structure of a protein can be derived from the C^α and possibly C^β chemical shifts,[5] information on conformational equilibria and dynamic processes in macromolecular structure can be obtained from amide proton exchange measurements, spin−spin relaxation, spin−lattice relaxation, and ^{15}N−^{1}H NOE measurements,[3,6] and unique information on

solvation may be obtained by NMR.[7] To extend such studies to larger particle sizes one therefore needs techniques for obtaining resonance assignments, in addition to the ability of recording high-quality correlation spectra, as has been achieved with transverse relaxation-optimized spectroscopy (TROSY)[8,9] and cross-correlated relaxation-enhanced polarization transfer (CRINEPT).[10] The incorporation of TROSY into triple resonance NMR experiments that are commonly used for the sequential assignment of ^{13}C,^{15}N-labeled or ^{2}H,^{13}C,^{15}N-labeled proteins resulted in up to 3-fold sensitivity gains for the individual ^{15}N−^{1}H groups of a 23 kDa protein when compared to the corresponding conventional NMR experiments.[11−14] Moreover, model calculations led us to predict much larger gains for TROSY-type triple resonance experiments when used with larger molecular sizes.[11]

This paper now documents the use of TROSY-type triple resonance experiments for the complete sequential assignment of a 121-residue polypeptide chain in a uniformly ^{2}H,^{13}C,^{15}N-labeled protein of size 110 kDa, 7,8-dihydroneopterin aldolase (DHNA) from *Staphylococcus aureus*,[15] demonstrating that the

---

* Address correspondence to this author.

† Eidgenössische Technische Hochschule Hönggerberg.

‡ F. Hoffmann-La Roche Ltd.

§ Current address: BRUKER Ltd., Industriestrasse 26, CH-8117 Fällanden, Switzerland.

(1) Abbreviations: 3D, three-dimensional; CRINEPT, cross correlated relaxation-enhanced polarization transfer; ct, constant-time; DHNA, 7,8-dihydroneopterin aldolase; NMR, nuclear magnetic resonance; NOE, nuclear Overhauser effect; rf, radio frequency; NOESY, NOE spectroscopy; TROSY, transverse relaxation-optimized spectroscopy.

(2) Wüthrich, K.; Wider, G.; Wagner, G.; Braun, W. *J. Mol. Biol.* **1982**, *155*, 311−319.

(3) Wüthrich, K. *NMR of Proteins and Nucleic Acids*; Wiley: New York, 1986.

(4) Shuker, S. B.; Hajduk, P. J.; Meadows, R. P.; Fesik, S. W. *Science* **1996**, *274*, 1531−1534.

(5) Spera, S.; Bax, A. *J. Am. Chem. Soc.* **1991**, *113*, 5490−5492. Wishart, D. S.; Sykes, B. D.; Richards, F. M. *J. Mol. Biol.* **1991**, *222*, 311−333. Luginbühl, P.; Szyperski, T.; Wüthrich, K. *J. Magn. Reson. B* **1995**, *109*, 229−233.

(6) Wider, G. *Prog. NMR Spectrosc.* **1998**, *32*, 193−275.

(7) Otting, G.; Liepinsh, E.; Wüthrich, K. *Science* **1991**, *254*, 974−980.

(8) Pervushin, K.; Riek, R.; Wider, G.; Wüthrich, K. *Proc. Natl. Acad. Sci. U.S.A.* **1997**, *94*, 12366−12371.

(9) Wüthrich, K. *Nature Struct. Biol.* **1998**, *5*, 492−495.

(10) Riek, R.; Wider, G.; Pervushin, K.; Wüthrich, K. *Proc. Natl. Acad. Sci. U.S.A.* **1999**, *96*, 4918−4923.

(11) Salzmann, M.; Pervushin, K.; Wider, G.; Senn, H.; Wüthrich K. *Proc. Natl. Acad. Sci. U.S.A.* **1998**, *95*, 13585−13590.

(12) Salzmann, M.; Wider, G.; Pervushin, K.; Senn, H.; Wüthrich K. *J. Am. Chem. Soc.* **1999**, *121*, 844−848.

(13) Salzmann, M.; Pervushin, K.; Wider, G.; Senn, H.; Wüthrich K. *J. Biomol. NMR* **1999**, *14*, 85−88.

(14) Salzmann, M.; Wider, G.; Pervushin, K.; Wüthrich, K. *J. Biomol. NMR* **1999**, *15*, 182−185.

(15) Hennig, M.; D'Arcy, A.; Hampele, I. C.; Page, M. G. P.; Oefner, C.; Dale, G. E. *Nature Struct. Biol.* **1998**, *5*, 357−362.

sequence-specific NMR assignment of polypeptide backbone resonances in particle sizes exceeding a molecular mass of 100 000 Da has become a reality with the advent of TROSY. Based on nearly complete sets of $^{13}C^\alpha$ and $^{13}C^\beta$ chemical shifts and on $^1H-^1H$ nuclear Overhauser effects (NOE) detected with [$^1H,^1H$]-NOESY-[$^{15}N,^1H$]-TROSY experiments,[16] which also contributed in important ways to the completion of the sequence-specific NMR assignments,[3] the regular secondary structures in the solution conformation of the DHNA octamer are compared with the crystal structure.[15]

Materials and Methods

Staphylococcus aureus 7,8-dihydroneopterin aldolase (DHNA) was overexpressed in *E.coli* M15(pRep4) harboring a pSaDHNA plasmid. Cells that had previously been adapted to ^2H_2O in minimal medium were grown at 37 °C in 1.5 L of labeled minimal medium in ^2H_2O (>99.8%) containing 0.8 g/L of $^{15}NH_4Cl$ (>98% ^{15}N) and 3.3 g/L of [$^2H_7,^{13}C_6$]-glucose (>97% ^2H, >98% ^{13}C), induced with isopropyl-β-D-thiogalactopyranoside and harvested by centrifugation. The cells were resuspended in lysis buffer (25 mM TRIS at pH 7.5, 50 mM NaCl, 5% glycerol, 10% saccharose, 1 mM EDTA, 4 tablets of protease inhibitor cocktail per liter from Boehringer, Art. No. 1836145) and subsequently disrupted (1 g cell mass/10 mL of buffer) using a cell homogenizer (Rannie). After centrifugation, the supernatant was filtered through a 0.2 μm filter (Gelman, VacuCap 60) and the filtrate was concentrated 10-fold using a 30 kD ultrafiltration membrane (Millipore). The first purification step was by anion-exchange chromatography (Fractogel-EMD TMAE, Merck) in 25 mM BICINE buffer, pH 7.0 (5% glycerol, 1 tablet of protease inhibitor cocktail/L), using a 1 cm × 15 cm column. The aldolase was eluted with the same buffer containing 1 M NaCl by a nonlinear gradient: 0−10% in 1.5 column volumes (CV), 10−35% in 13.5 CV, 35−100% in 3 CV. The second purification step was by size-exclusion-chromatography (Superdex-200, Pharmacia; HR 10/30 FPLC column) in 75 mM ammonium−$^2H_3$−acetate buffer at pH 6.5 (>98% ^2H). The purified protein solution was concentrated by ultrafiltration to the desired NMR concentration (0.5 mM). To obtain the NMR sample, 5% ^2H_2O was added to the solution.

The mass spectrometry analysis of the [$^2H,^{13}C,^{15}N$]-labeled aldolase octamer used for the NMR experiments showed a molecular mass per subunit of 15 227.6 Da. Using experimental data from $^{13}C,^{15}N$-labeling of DHNA which showed an isotope enrichment of 99% for ^{15}N and 98% for ^{13}C, we calculated that the ^2H enrichment was at least 95%.

All NMR spectra were recorded at 20 °C with the same DHNA sample. The [$^{15}N,^1H$]-TROSY-HNCA,[11] [^{13}C]-ct-[$^{15}N,^1H$]-TROSY-HNCA,[13] [$^{15}N,^1H$]-TROSY-HNCACB,[12] [$^{15}N,^1H$]-TROSY-HNCO,[11] and [$^1H,^1H$]-NOESY-[$^{15}N,^1H$]-TROSY[16] experiments were recorded on a Bruker-DRX750 MHz spectrometer using a triple-resonance probe with an actively shielded *z*-gradient coil and four radio frequency (rf) channels for generating the ^1H, ^2H, ^{13}C, and ^{15}N rf pulses. The [$^{15}N,^1H$]-TROSY-HN(CO)CA[12] experiment was measured on a Bruker-DRX500 MHz spectrometer with the same configuration as the DRX750. In this experiment, fast transverse ^{13}CO relaxation due CSA leads to signal decrease with increasing magnetic field strength, and actually deteriorates the spectrum already at 500 MHz.

In the triple resonance experiments the optimal duration of the magnetization transfer periods between ^{13}C and ^{15}N was found to be about 17 ms. Hence the ct evolution time for ^{15}N also had this value, which provides for sufficient resolution in the ^{15}N dimension. The following parameter settings were used for the individual experiments. *[$^{15}N,^1H$]-TROSY-HNCA*: data size $42(t_1) \times 40(t_2) \times 1024(t_3)$ complex points; $t_{1max}(^{15}N) = 17.4$ ms, $t_{2max}(^{13}C) = 8.0$ ms, $t_{3max}(^1H) = 75.6$ ms; number of scans accumulated per (t_1,t_2)-increment (NS) = 96, interscan delay 0.92 s, total measuring time 156 h. *[^{13}C]-ct-[$^{15}N,^1H$]-TROSY-HNCA*: $42(t_1) \times 128(t_2) \times 1024(t_3)$ complex points; $t_{1max}(^{15}N) = 17.4$ ms, $t_{2max}(^{13}C) = 25.6$ ms, $t_{3max}(^1H) = 75.6$ ms; NS = 16, interscan delay 1.0 s, total measuring time 96 h. *[$^{15}N,^1H$]-TROSY-HNCACB*:

$42(t_1) \times 44(t_2) \times 1024(t_3)$ complex points; $t_{1max}(^{15}N) = 17.4$ ms, $t_{2max}(^{13}C) = 4.6$ ms, $t_{3max}(^1H) = 75.6$ ms; NS = 80, interscan delay 0.96 s, total measuring time 144 h. *[$^{15}N,^1H$]-TROSY-HNCO*: $42(t_1) \times 32(t_2) \times 1024(t_3)$ complex points; $t_{1max}(^{15}N) = 17.4$ ms, $t_{2max}(^{13}C) = 12.8$ ms, $t_{3max}(^1H) = 75.6$ ms; NS = 24, interscan delay 1.0 s, total measuring time 36 h. *[$^1H,^1H$]-NOESY-[$^{15}N,^1H$]-TROSY*: $30(t_1) \times 128(t_2) \times 1024(t_3)$ complex points; $t_{1max}(^{15}N) = 15.0$ ms, $t_{2max}(^1H) = 24.4$ ms, $t_{3max}(^1H) = 105$ ms; NS = 16, NOE mixing time 300 ms, interscan delay 1.0 s, total measuring time 68 h. *[$^{15}N,^1H$]-TROSY-HN(CO)CA*: $27(t_1) \times 28(t_2) \times 1024(t_3)$ complex points; $t_{1max}(^{15}N) = 16.9$ ms, $t_{2max}(^{13}C) = 8.4$ ms, $t_{3max}(^1H) = 114$ ms; NS = 48, interscan delay 1.0 s, total measuring time 48 h. Prior to Fourier transformation the data matrices were multiplied with a 60°-shifted sine bell window in the acquisition dimension and a 75°-shifted sine bell window in the two indirect dimensions.[17] The programs PROSA[18] and XEASY[19] were used for data processing and spectral analysis, respectively.

Results and Discussion

All NMR experiments in this paper were performed with the same sample of a 0.5 mM solution of uniformly $^2H,^{13}C,^{15}N$-labeled *S. aureus* DHNA (7,8-dihydroneopterin aldolase) in 95% H_2O/5% D_2O at pH 6.5 and $T = 20$ °C (see also the Materials and Methods section). The sequential assignment of the 121-residue polypeptide chain in this octameric 110 kDa protein was performed using a set of TROSY-type triple resonance experiments,[11−14] which yielded the chemical shift assignments for the backbone amide groups, $^1H^N$ and ^{15}N, the backbone carbons, $^{13}C^\alpha$ and ^{13}CO, as well as most of the side chain $^{13}C^\beta$ atoms. The chemical shift lists have been deposited at BioMag-ResBank (www.bmrb.wisc.edu) under the BMRB accession number 4573.

From previous studies with smaller proteins[12] and from model calculations[11] a more than 10-fold sensitivity gain has been anticipated to result from the use of TROSY in triple resonance experiments with structures of molecular mass around 100 kDa. To verify this prediction with experimental data, a conventional HNCA spectrum[21] and a [$^{15}N,^1H$]-TROSY-HNCA spectrum[11] were measured with otherwise identical conditions (Figure 1). A 20- to 50-fold sensitivity gain, depending on the residue considered, was achieved using [$^{15}N,^1H$]-TROSY-HNCA (Figure 1, c and d), and nearly all expected cross-peaks could be observed. With the conventional scheme,[21] the HNCA cross-peaks could be unambiguously detected for only 7 out of the 121 residues of DHNA, and only the apparently highly flexible C-terminal Lys 121 yielded strong sequential and intraresidual peaks (Figure 1b).

As is common in sequential assignments of $^{13}C,^{15}N$-labeled proteins,[20] the HNCA experiment had a key role also in the present project. For the assignments we recorded a [$^{15}N,^1H$]-TROSY-HNCA[11] data set with twice the measuring time of the experiment in Figure 1 (Figure 2). For a large fraction of the polypeptide chain the peaks were sufficiently well resolved for establishing the sequential connectivities, which are indicated by dotted lines in Figures 2 and 3a. In these two illustrations the strip of Arg 11 is the only one where no reliable sequential assignment was possible due to signal overlap. The distinction between intraresidual and sequential peaks in the HNCA spectrum was in most instances determined from the relative signal intensities of the sequential and intraresidual peaks, since

(16) Pervushin, K.; Wider, G.; Riek, R.; Wüthrich, K. *Proc. Natl. Acad. Sci. U.S.A.* **1999**, *96*, 9607−9612. Zhu, G.; Kong, X. M.; Sze, K. H. *J. Biomol. NMR* **1999**, *13*, 77−81.

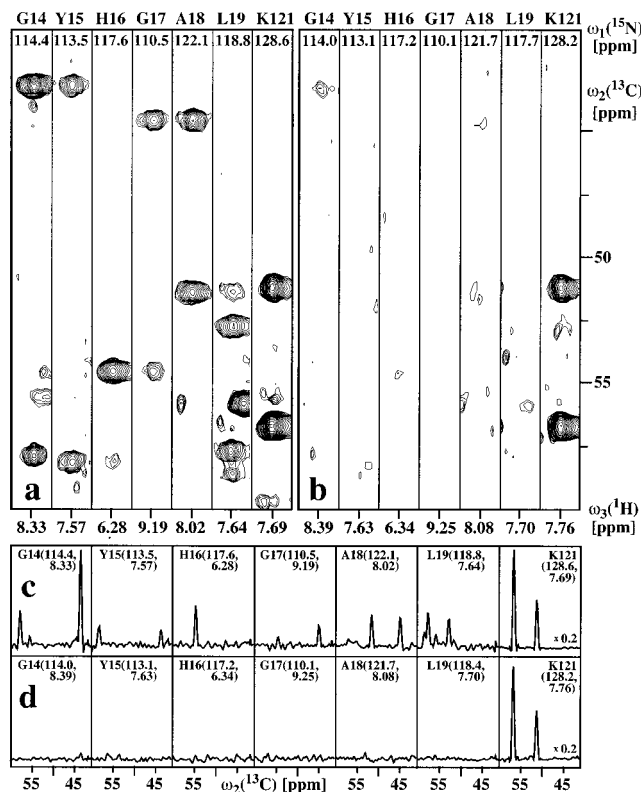(17) DeMarco, A.; Wüthrich, K. *J. Magn. Reson.* **1976**, *24*, 201−204.
(18) Güntert, P.; Dötsch, V.; Wider, G.; Wüthrich, K. *J. Biomol. NMR* **1992**, *2*, 619−629.
(19) Bartels, C.; Xia, T.; Billeter, M.; Güntert, P.; Wüthrich, K. *J. Biomol. NMR* **1995**, *5*, 1−10.
(20) Bax, A.; Grzesiek, S. *Acc. Chem. Res.* **1993**, *26*, 131−138.
(21) Grzesiek, S.; Bax, A. *J. Magn. Reson.* **1992**, *96*, 432−440.

Figure 1. Comparison of corresponding [ω_2(^{13}C), ω_3(^{1}H)] strips from two 3D HNCA experiments recorded with a 0.5 mM solution of the uniformly ^{2}H,^{13}C,^{15}N-labeled octameric 110 kDa *Staphylococcus aureus* 7,8-dihydroneopterin aldolase (DHNA) (the molar concentration is for the octamer, the sample contained 50 mg of DHNA per ml): (a) [^{15}N,^{1}H]-TROSY-HNCA[11]and (b) conventional HNCA[21] adapted to the scheme employed for panel a by using water flip-back pulses,[22] a WATERGATE sequence[23] for residual solvent suppression before acquisition, and off-resonance ^{13}CO SEDUCE[24] decoupling. For both spectra the experimental conditions described in the Material and Methods section for [^{15}N,^{1}H]-TROSY-HNCA were modified in that only 48 scans were accumulated per (t_1,t_2)-increment, resulting in 78 h total measuring time. The strips were taken at the ^{15}N chemical shifts that have in the present paper been assigned to the residues 14−19 and the C-terminal Lys 121. They are centered about the corresponding amide proton chemical shifts and have a width of 131 Hz along ω_3-(^{1}H). The panels c and d show cross-sections along the ω_2(^{13}C) axis through the peaks in panels a and b, respectively. In each panel the intraresidual peak is identified by the one-letter amino acid symbol and the residue number, and the ω_1(^{15}N) and ω_3(^{1}H) chemical shifts are indicated in parentheses.

the sequential peaks are normally less intense due to the slightly smaller ^{2}J(^{15}N,^{13}C$^\alpha$) scalar coupling constant for the sequential connectivity when compared to the intraresidual ^{1}J(^{15}N,^{13}C$^\alpha$) coupling. In cases where the sequential and the intraresidual peaks in the HNCA spectrum were of near-equal intensity, e.g., for Lys 68 and Ala 69 (Figure 3a), a 3D [^{15}N,^{1}H]-TROSY-HN-(CO)CA[12] spectrum was consulted (Figure 3b), which only shows the sequential cross-peaks.

The aforementioned residue Arg 11 (Figure 2) is one of several residues in DHNA that show overlap in the ^{13}C dimension of the [^{15}N,^{1}H]-TROSY-HNCA spectrum. To resolve the ensuing ambiguities, 3D [^{15}N,^{1}H]-TROSY-HNCACB[12] and 3D [^{13}C]-ct-[^{15}N,^{1}H]-TROSY-HNCA[13] experiments were used. Figure 4 presents [ω_2(^{13}C),ω_3(^{1}H)] strips from a 3D [^{15}N,^{1}H]-TROSY-HNCACB spectrum, taken at the ^{15}N chemical shifts of residues 8−14. The sequential assignment for Arg 11 was readily obtained via the ^{13}C$^\beta$ chemical shifts, which are nicely
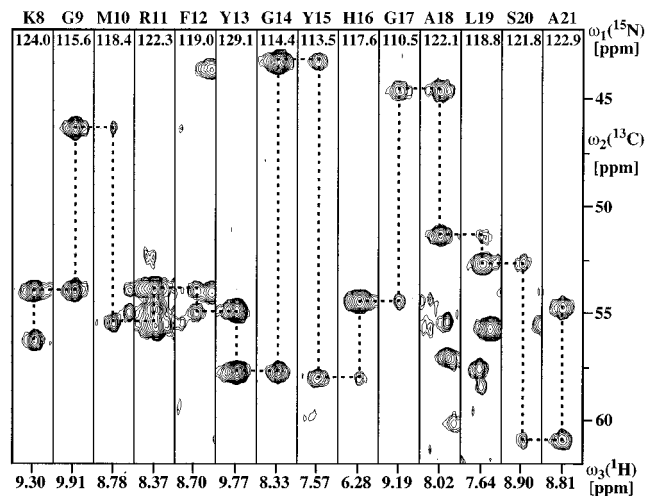
Figure 2. Similar presentation as in Figure 1a of [ω_2(^{13}C), ω_3(^{1}H)] strips from the 3D [^{15}N,^{1}H]-TROSY-HNCA[11] experiment with the DHNA sample of Figure 1 that was used for sequential assignment (the experimental parameters are given in the Material and Methods section). At the top of each strip the sequence-specific assignment is indicated by the one-letter amino acid symbol and the residue number in the amino acid sequence. The broken line indicates the assignment pathway through the intraresidual and sequential HNCA connectivities.
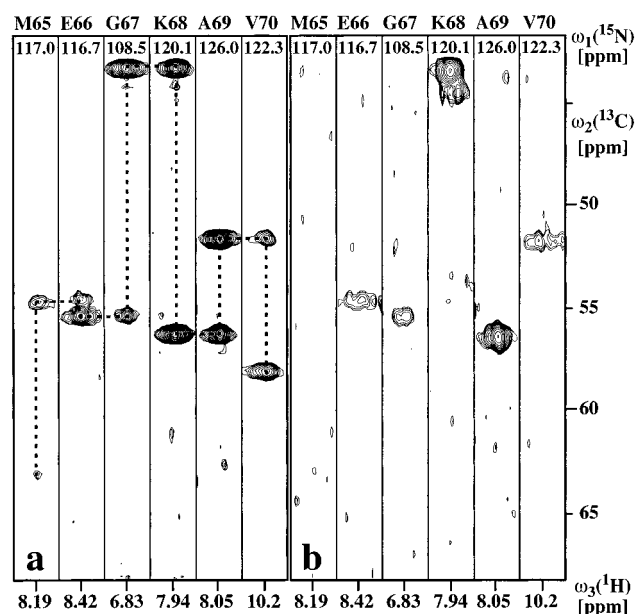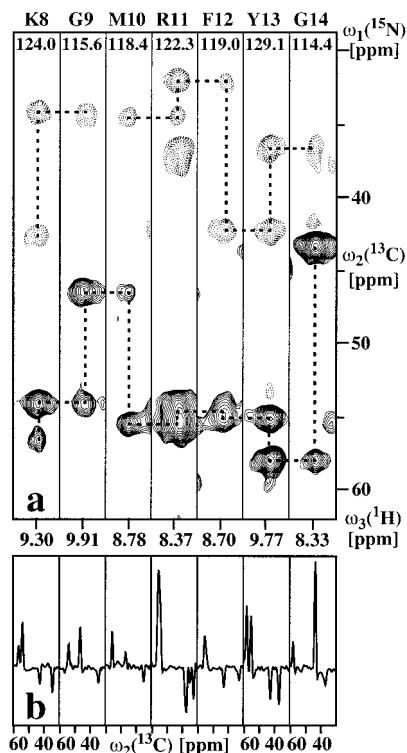

Figure 3. [ω_2(^{13}C), ω_3(^{1}H)] strips from 3D [^{15}N,^{1}H]-TROSY-HNCA[11] (a) and 3D [^{15}N,^{1}H]-TROSY-HN(CO)CA[12] (b) experiments recorded with the DHNA sample of Figure 1. Same presentation as in Figure 2. Some of the connectivities indicated in panel a were supported by the data in panel b (see text).

dispersed for this residue (Figure 4), and unambiguous assignments were obtained for several other residues. All the ^{13}C$^\beta$ resonances could not, however, be observed in the [^{15}N,^{1}H]-TROSY-HNCACB spectrum due to the inherently lower sensitivity when compared with [^{15}N,^{1}H]-TROSY-HNCA. Some missing sequential connectivities could then be established via the ^{13}C$^\alpha$ chemical shifts based on the 4-fold higher resolution along the ω_2(^{13}C) dimension achieved in a [^{13}C]-ct-[^{15}N,^{1}H]-TROSY-HNCA spectrum. These data for DHNA have previously been presented elsewhere.[13]
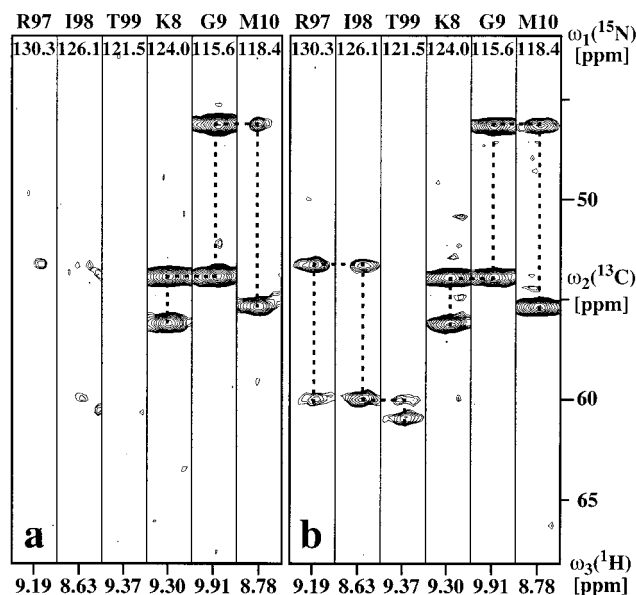
In the early phase of the project, progress was slow because of missing [ω_2(^{13}C),ω_3(^{1}H)] strips. The protein expression and purification was entirely performed in deuterated media and all

Figure 4. $[\omega_2(^{13}C), \omega_3(^1H)]$ strips from a 3D $[^{15}N,^1H]$-TROSY-HNCACB[12] spectrum recorded with the DHNA sample of Figure 1. The $^{13}C^\alpha$ resonances are positively phased and drawn with solid contours and the $^{13}C^\beta$ resonances show opposite sign and are drawn with dotted contours; the strips have a width of 131 Hz along $\omega_3(^1H)$. Same presentation as in Figure 2, whereby two suites of dashed lines indicate sequential connectivities observed independently for the $^{13}C^\alpha$ and $^{13}C^\beta$ resonances. (b) Cross-sections along the $\omega_2(^{13}C)$ axis through the peaks in panel a.

amide deuterons had not been sizably exchanged by protons when the initial experiments in H_2O solution were recorded. In particular, very weak signals due to incomplete $^2H/^1H$ exchange were obtained for some of the residues in regular secondary structure elements. Figure 5 shows $[\omega_2(^{13}C),\omega_3(^1H)]$ strips from two 3D $[^{15}N,^1H]$-TROSY-HNCA spectra that were recorded either shortly after the sample preparation (Figure 5a) or later-on after the sample had been at 20 °C for several weeks and at 4 °C for about two additional months (Figure 5b). The strips were taken at the ^{15}N chemical shifts of residues 8−10 and 97−99, respectively, which are all located in β-sheet regions of DHNA. For the amino acid residues 97−99, slow amide proton exchange is clearly apparent, whereas the amino acid residues 8−10 were already fully protonated in the freshly prepared sample. Similar observations have of course been described for other systems,[25] and the partial exchange of the amide protons in freshly prepared D_2O solutions was actually a great help in the initial sequential resonance assignments.[26] We emphasize this difficulty here, since it gives an indication that there will be advantages in expressing high molecular weight systems in

(22) Grzesiek, S.; Bax, A. *J. Am. Chem. Soc.* **1993**, *115*, 12593−12594.
(23) Piotto, M.; Saudek, V.; Sklenar, V. J. *J. Biomol. NMR* **1992**, *2*, 661−665.
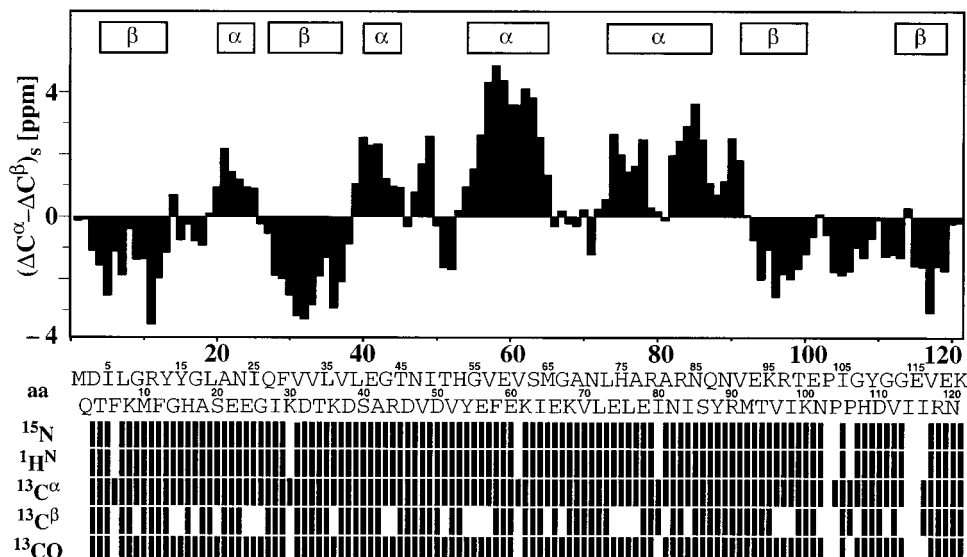(24) McCoy, M. A.; Mueller, L. *J. Am. Chem. Soc.* **1992**, *114*, 2108−2112.
(25) Gardner, K. H.; Zhang, X.; Gehring, K.; Kay, L. E. *J. Am. Chem. Soc.* **1998**, *120*, 11738−11748.
(26) Dubs, A.; Wagner, G.; Wüthrich, K. *Biochim. Biophys. Acta* **1979**, *577*, 177−194. Wagner, G.; Anil-Kumar; Wüthrich, K. *Eur. J. Biochem.* **1981**, *114*, 375−384.

Figure 5. Comparison of corresponding $[\omega_2(^{13}C), \omega_3(^1H)]$ strips from two 3D $[^{15}N,^1H]$-TROSY-HNCA experiments[11] with the DHNA sample of Figure 1: (a) recorded shortly after the sample preparation and (b) recorded three months after sample preparation using identical experimental parameters. Same presentation as in Figure 2, except that the width of the strips along $\omega_3(^1H)$ is 79 Hz. The $^2H/^1H$ amide proton exchange for residues 8−10 was virtually complete in the freshly prepared sample, whereas no or only weak signals were detected for residues 97−99 because of slow $^2H/^1H$ exchange.

unfolded form in inclusion bodies and refold in H_2O to obtain uniform protonation of the amide groups.

The ^{13}C chemical shifts obtained for DHNA were used to characterize the secondary structure of the protein by analysis of the deviations, ΔC^α and ΔC^β, of the observed $^{13}C^\alpha$ and $^{13}C^\beta$ chemical shifts from their residue-dependent random coil values.[3,27] In Figure 6, the parameter $(\Delta C^\alpha - \Delta C^\beta)$[28] is plotted for the entire polypeptide chain of the DHNA monomers. Consecutive positive or negative $(\Delta C^\alpha - \Delta C^\beta)$ values identify α-helical or β-sheet regions, respectively, and the regular secondary structures thus identified correlate well with those in the X-ray structure of DHNA.[15] The only apparent discrepancy is that the NMR data for residues 104−109 indicate β-sheetlike conformation (Figure 6), although no β-strand was identified in the X-ray structure. Inspection of the X-ray structure of the DHNA octamer then revealed that there is nonetheless an extended conformation for these residues, with several intersubunit hydrogen bonds between amide hydrogens and carbonyl carbons, which provides a satisfactory rationale for the NMR data. The chemical shift assignments summarized in Figure 6 were obtained with the experiments of Figures 2−5 and a $[^{15}N,^1H]$-TROSY-HNCO measurement,[11] which again demonstrates the striking advance achieved with the use of TROSY (Figure 7).

The sequential assignment and the secondary structure characterization of DHNA was independently supported, and in some instances extended, by the analysis of NOE data obtained with a 3D $[^1H,^1H]$-NOESY-$[^{15}N,^1H]$-TROSY experiment (Figure 8).[16] Especially for the regular secondary structure elements the $[^1H,^1H]$-NOESY-$[^{15}N,^1H]$-TROSY spectrum was

(27) Richarz, R.; Wüthrich, K. *Biopolymers* **1978**, *17*, 2133-2141. Wishart, D. S.; Sykes, B. D. *J. Biomol. NMR* **1994**, *4*, 171−180.
(28) Metzler, W. J.; Constantine, K. L.; Friedrichs, M. S.; Bell, A. J.; Ernst, E. G.; Lavoie, T. B.; Mueller, L. *Biochemistry* **1993**, *32*, 13818−13829.

Figure 6. Survey of the NMR assignments by the triple resonance experiments for the 121-residue polypeptide chain in the 110 kDa DHNA octamer, and identification of secondary structure elements in DHNA by ^{13}C chemical shift analysis.[5] The amino acid sequence is indicated in the double line marked aa, and the residues for which the[15]N, [1]H[N], [13]C[α], [13]C[β], and [13]CO chemical shifts, respectively, have been assigned are indicated by the vertical black bars below the sequence. In the top panel the values of $(\Delta C^\alpha - \Delta C^\beta)$ are plotted versus the amino acid sequence, where ΔC^α and ΔC^β were obtained by subtracting the corresponding random coil [13]C[α] and [13]C[β] chemical shifts[27] from the shifts measured in the spectra of DHNA.[5] The value $(\Delta C^\alpha - \Delta C^\beta)$ for a particular residue i represents an average over three consecutive residues: $(\Delta C^\alpha - \Delta C^\beta)_i = (\Delta C^\alpha_{i-1} + \Delta C^\alpha_i + \Delta C^\alpha_{i+1} - \Delta C^\beta_{i-1} - \Delta C^\beta_i - \Delta C^\beta_{i+1})/3$.[28] The locations of the α-helices and β-sheets in the X-ray crystal structure of DHNA[15] are indicated by the open rectangles at the top of the figure.
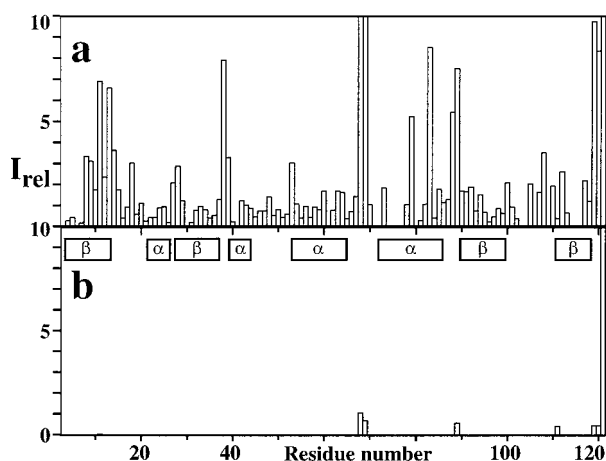

Figure 7. Comparison of the relative signal intensities, I_{rel}, obtained in 3D HNCO experiments recorded with and without TROSY using the DHNA sample of Figure 1: (a) [^{15}N,^{1}H]-TROSY-HNCO[11] and (b) conventional HNCO.[21] The conventional HNCO measurement has been adapted to the scheme used in panel a by the addition of water flip-back pulses,[22] and a WATERGATE sequence[23] for residual solvent suppression. Both spectra were recorded with the same experimental conditions and processed identically. The locations of the α-helical and β-sheet regions in the X-ray crystal structure of DHNA[15] are identified in panel b.

very useful for cross checking of the sequential assignments obtained from the 3D triple resonance spectra. In addition, by reference to the crystal structure of DHNA,[15] amide proton−amide proton NOE contacts across β-strands within one subunit, $d_{NN}(i,j)$,[3] could be assigned, such as between Lys 100 and Val 112, as well as intersubunit contacts, e.g., between the amide protons of Asp 110 of one subunit and Gly 9′ of a neighboring subunit, and similarly between Gly 111 and Lys 8′, where the distances $d_{NN}(i,j)$ in the DHNA X-ray structure are 4.4 and 3.2 Å, respectively.[15] Figure 9 presents a survey of the NOESY data for DHNA. The appearance of medium-range amide [1]H-
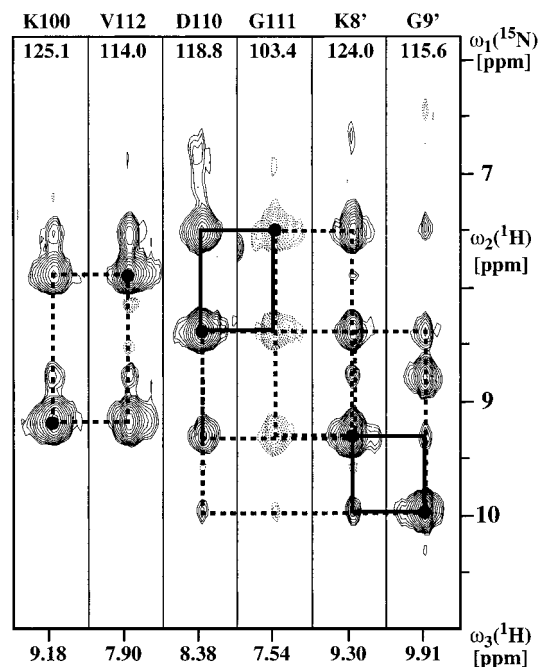
Figure 8. [ω_2(^{1}H), ω_3(^{1}H)] strips from a 3D [^{1}H,^{1}H]-NOESY-[^{15}N,^{1}H]-TROSY[16] experiment with the DHNA sample of Figure 1. The strips were taken at the ^{15}N chemical shifts of residues 100, 112, 110, 111, 8′, and 9′ and are centered about the corresponding [1]H[N] chemical shifts, and have a width of 164 Hz along ω_3(^{1}H); the residues K8′ and G9′ belong to a different subunit in the DHNA octamer than D110 and G111. At the top of each strip the sequence-specific assignments are indicated by the one-letter amino acid symbol and the residue number. Black dots indicate diagonal peaks, and the solid lines show the sequential NOE connectivities d_{NN} between D110 and G111, and between K8′ and G9′, respectively.[2,3] Dashed lines indicate $d_{NN}(i,j)$ cross-peaks either across β-strands, e.g., K100−V112, or between residues from different subunits of DHNA, e.g., D110−G9′ and G111−K8′. These long-range NOEs were assigned by reference to the crystal structure of DHNA.[15]
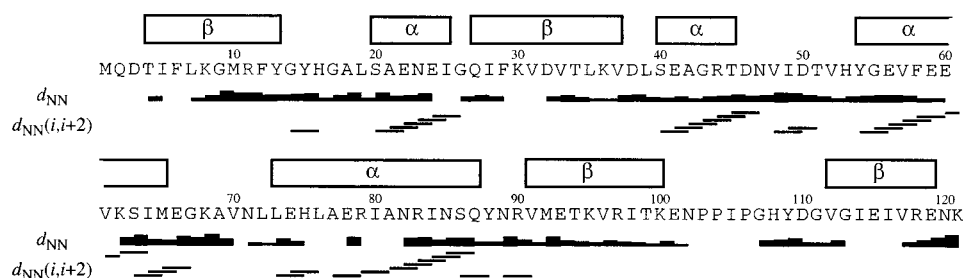
Figure 9. Survey of the sequential and medium-range NOE connectivities observed in DHNA. For the sequential NOEs, d_{NN}, the thickness of the line is proportional to the NOE intensity. The medium-range connectivities $d_{NN}(i,i+2)$ are indicated by lines covering the tripeptide segment that contains this NOE, which is indicative for the presence of an α-helix.[3] The locations of the α-helices and β-sheets in the X-ray crystal structure of DHNA are indicated by the bars above the sequence.[15]

amide ^{1}H NOEs, $d_{NN}(i,i+2)$,[3] is indicative of α-helical conformations, and these data coincide well with the positions of the α-helices in the crystal structure of DHNA.[15]

In conclusion, this paper demonstrates that sequence-specific NMR assignments and identification of the regular secondary structures can be achieved for uniformly ^{2}H,^{13}C,^{15}N-labeled proteins in particles with a molecular mass beyond 100 kDa when using TROSY-type NMR spectroscopy. The data presented in this paper also confirm our earlier prediction of quite staggering sensitivity gains of 1 to 2 orders of magnitude when TROSY-type triple resonance experiments are used with particle sizes of the order of 100 kDa.[11] For example, even for the most sensitive triple resonance experiment, HNCO, almost no signals were detectable in DHNA with the conventional experiment, whereas a nearly complete set of cross-peaks was detected with the [^{15}N,^{1}H]-TROSY-HNCO scheme[11] (Figure 7). Clearly, DHNA does not present a highly complex NMR spectrum, due to its 8-fold internal symmetry, and additional techniques, such as segmental isotope labeling,[29] will be needed to tackle the higher spectral crowding in large nonsymmetrical proteins. However, similar situations as with DHNA may be encountered,

for example, with labeled proteins of moderate size bound to unlabeled nucleic acids, or membrane proteins reconstituted and solubilized in lipid or detergent micelles of size about 100 kDa. For such systems backbone resonance assignments with the presently described techniques can provide the basis for a wide range of NMR measurements relating to functional properties, including studies of structure−activity relationships by investigating small-ligand binding with such complex systems.[4,30]

(29) Yamazaki, T.; Otomo, T.; Oda, N.; Kyogoku, Y.; Uegaki, K.; Ito, N.; Ishino, Y.; Nakamura, H. *J. Am. Chem. Soc.* **1998**, *120*, 5591−5592. Otomo, T.; Teruya, K.; Uegaki, K.; Yamazaki, T.; Kyogoku, Y. *J. Biomol. NMR* **1999**, *14*, 105−114.

(30) Wang, J.; Hinck, A. P.; Loh, S. N.; LeMaster, D. M.; Markley, J. L. *Biochemistry* **1992**, *31*, 921−936. Chen, Y.; Reizer, J.; Saier, H.; Fairbrother, W. J.; Wright, P. *Biochemistry* **1993**, *32*, 32−37.